



**The Abdus Salam  
International Centre for Theoretical Physics**



**2240-15**

**Advanced School on Scaling Laws in Geophysics: Mechanical and  
Thermal Processes in Geodynamics**

*23 May - 3 June, 2011*

**Derivation of thin viscous sheet equations**

G. Houseman  
*Univ. of Leeds*  
*UK*

Advanced School on  
Scaling Laws in Geophysics:  
Mechanical and Thermal Processes  
in Geodynamics

# Thin Viscous Sheet Model

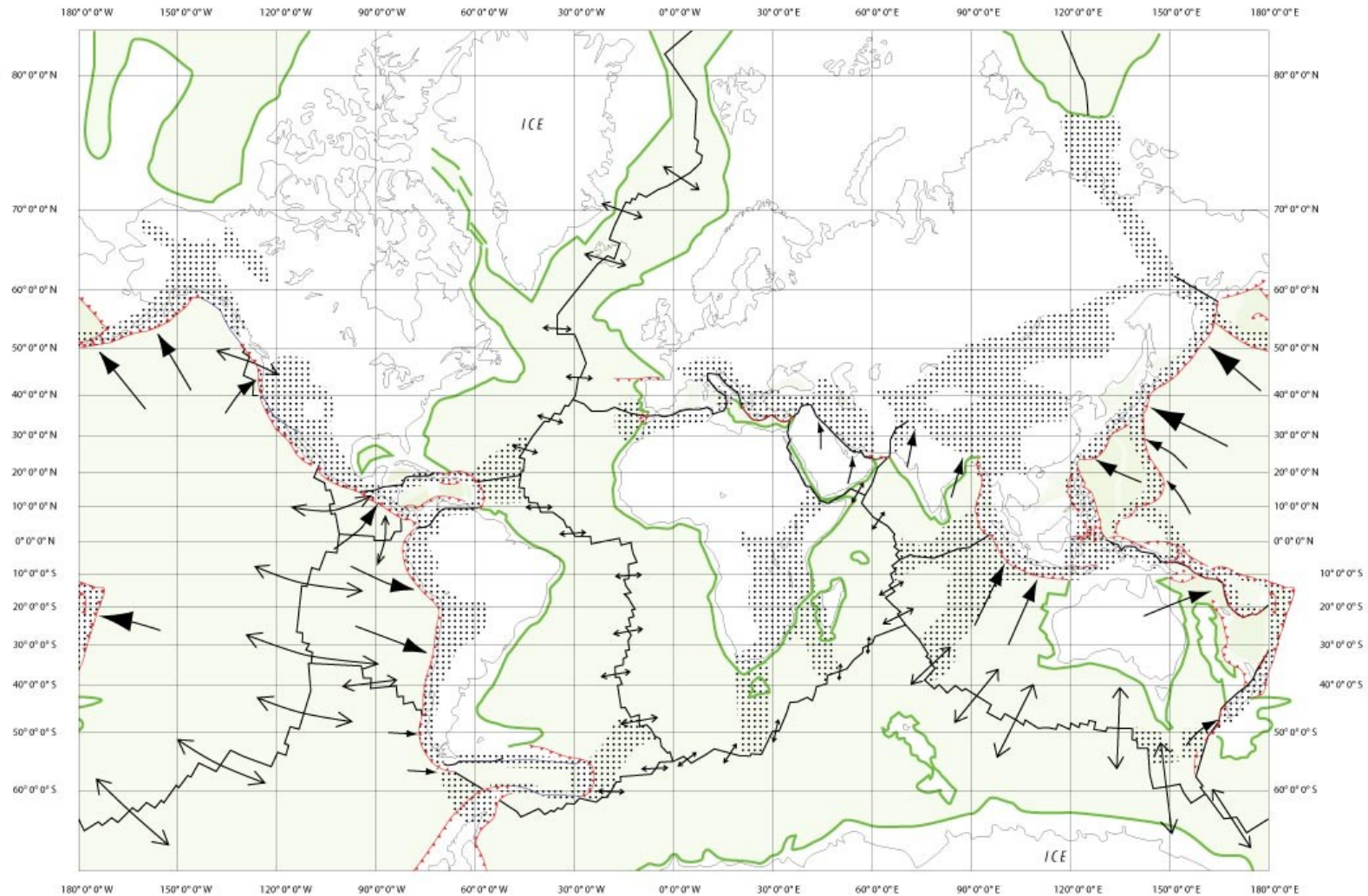
---

Greg Houseman

School of Earth and Environment  
University of Leeds, Leeds, LS2 9JT, UK  
[greg@earth.leeds.ac.uk](mailto:greg@earth.leeds.ac.uk)

# Regions of Diffuse Deformation

3.5  
Diffuse Plate  
Boundaries 1  
2-12-07 FINAL



Modified from Gordon & Stein 1992,  
Gordon 1995, 1998, 2000 and 2006

## Diffuse Deformation

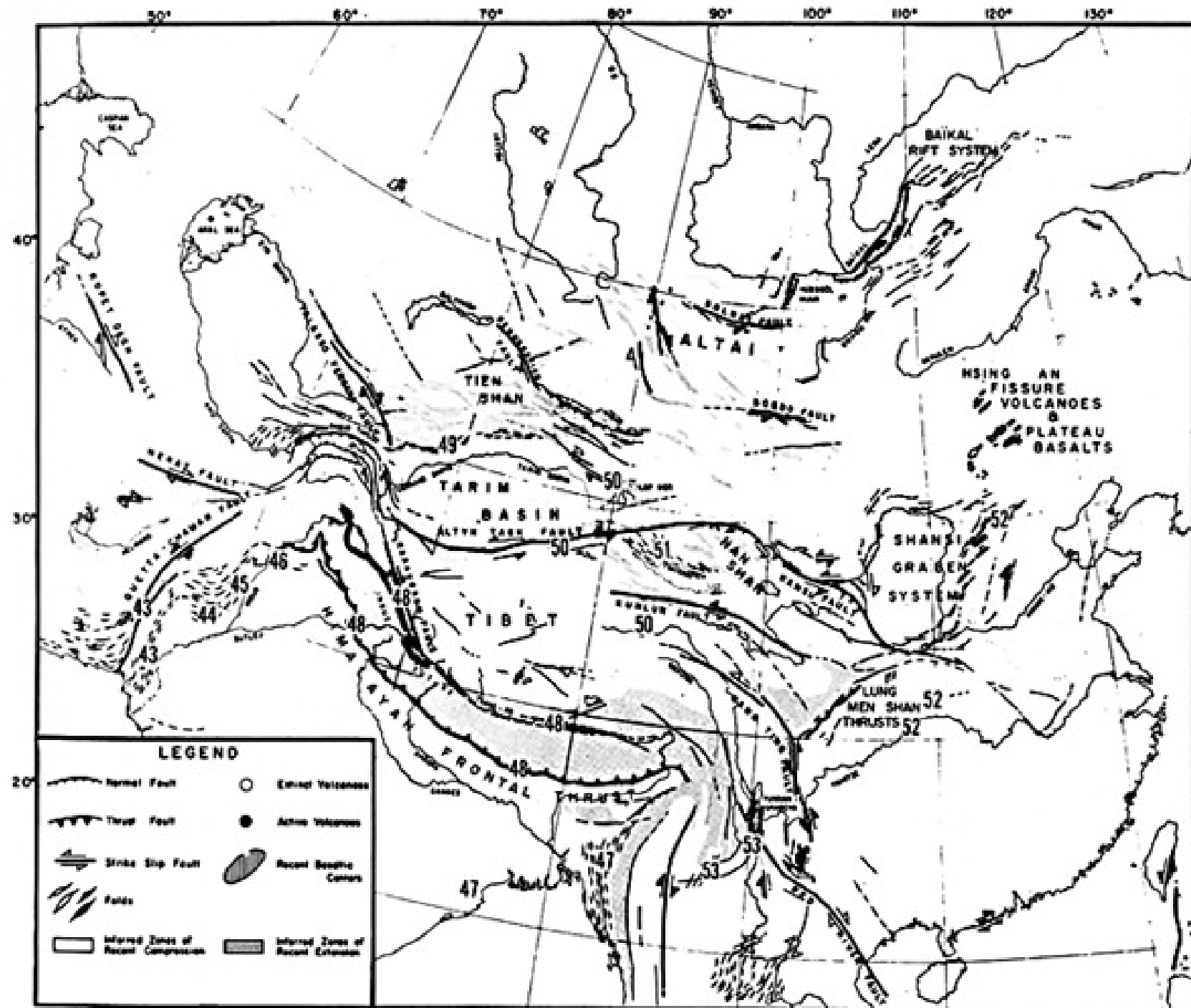
Plate Tectonics generally works - but not always. The idealized plate boundary (ridge, trench, or transform) is a narrow linear feature which absorbs all the relative motion between plates.

In fact, sometimes that relative movement produces strain over a large region, often referred to as a diffuse plate boundary. In such regions convergence is often associated with crustal thickening and mountain building, divergence with basin formation.

Seismic measurements and geomorphological measurements have been used to estimate strain rates where convergence is ongoing. Such estimates are confirmed by geodetic (GPS) measurements in recent years.

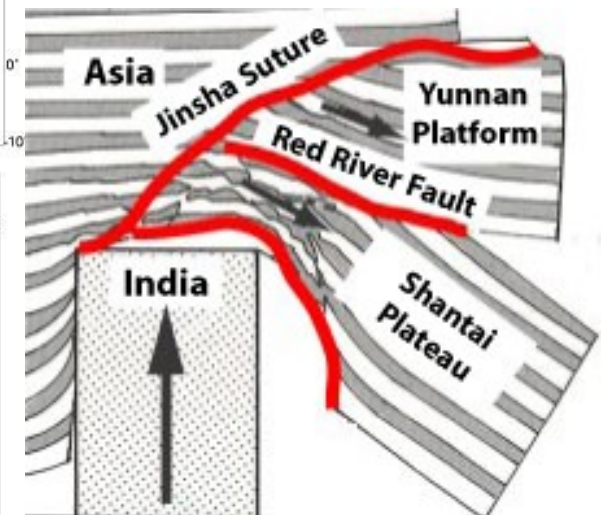
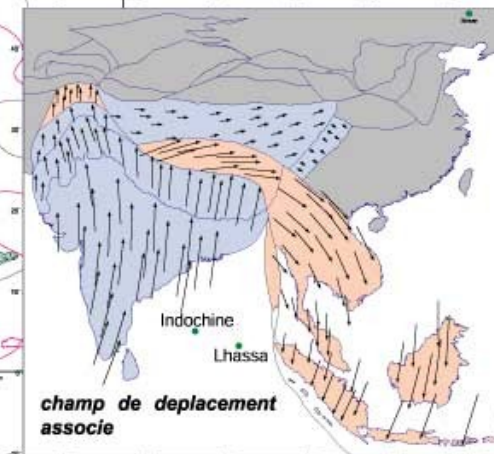
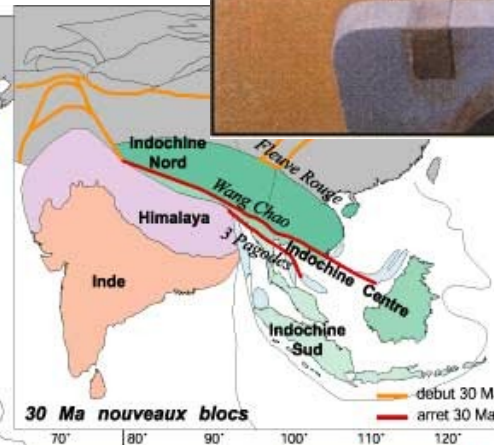
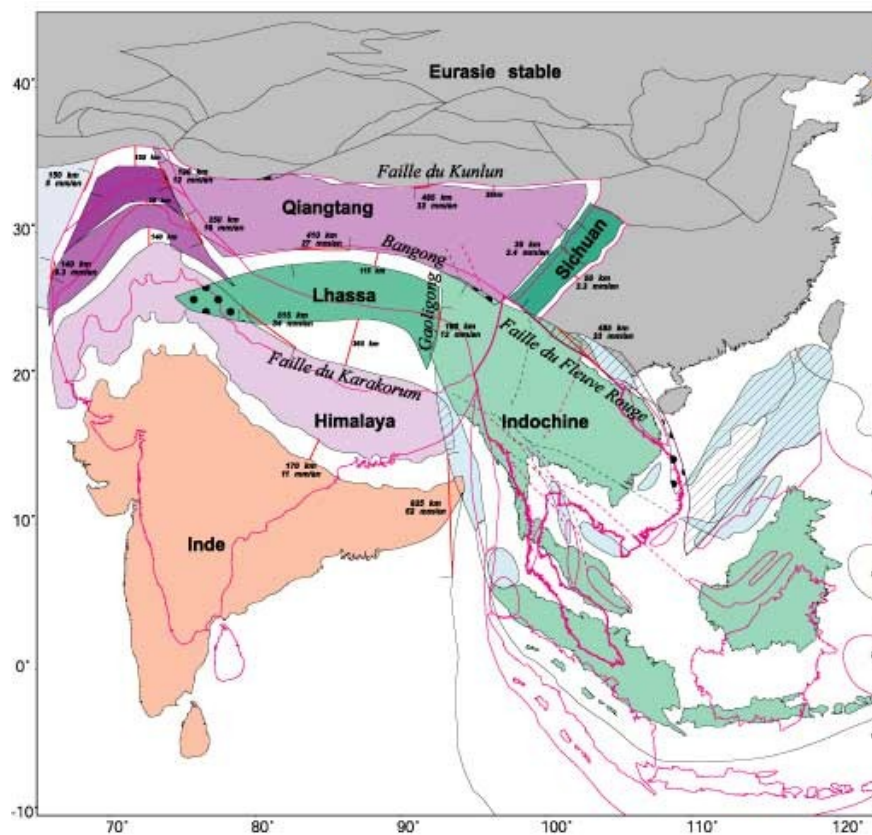
Argand described Alpine-Himalayan deformation in the 1920's. The topic was renewed in 1975 by Molnar and Tapponnier.

Molnar and Tapponnier, 1975

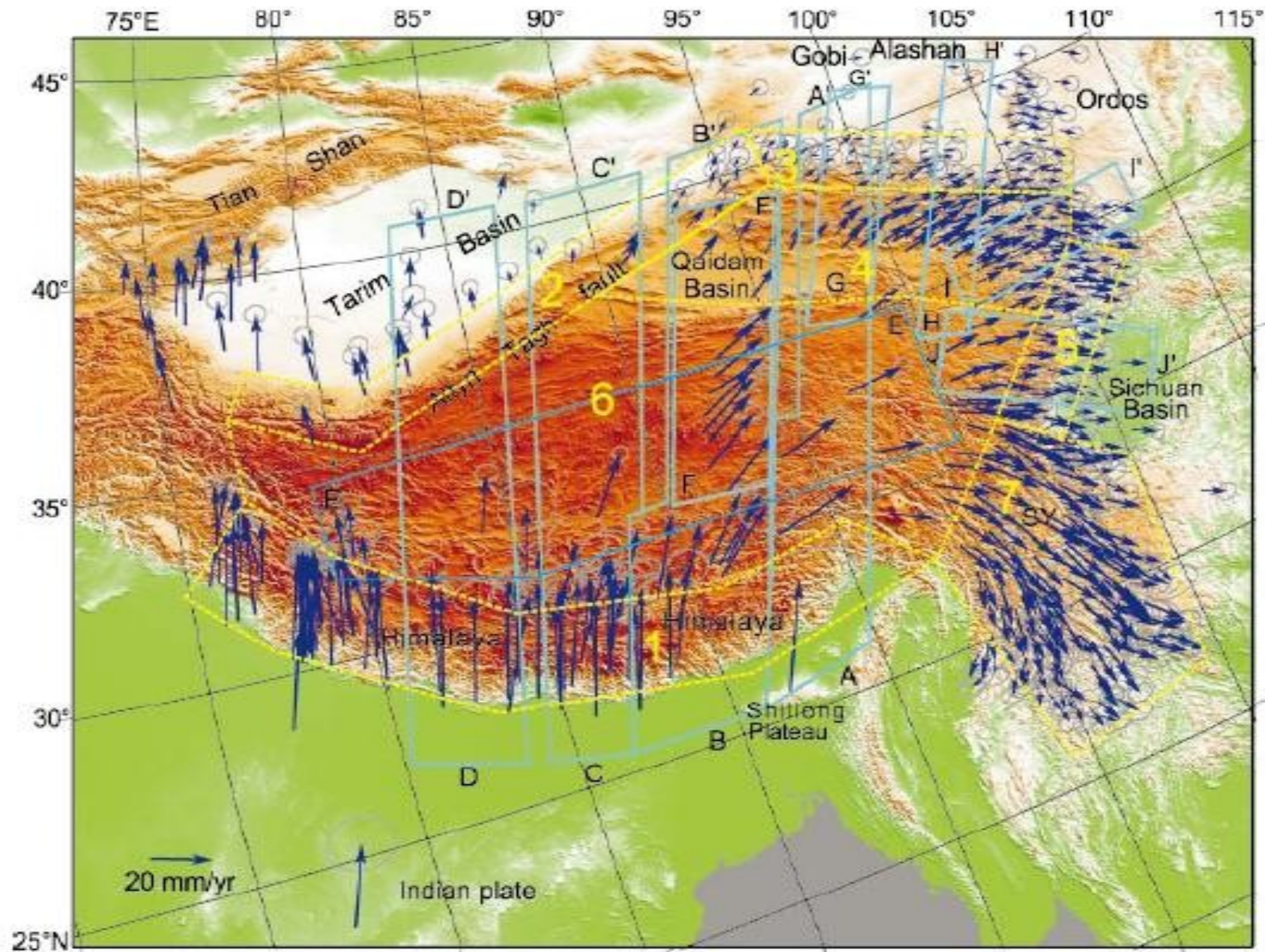


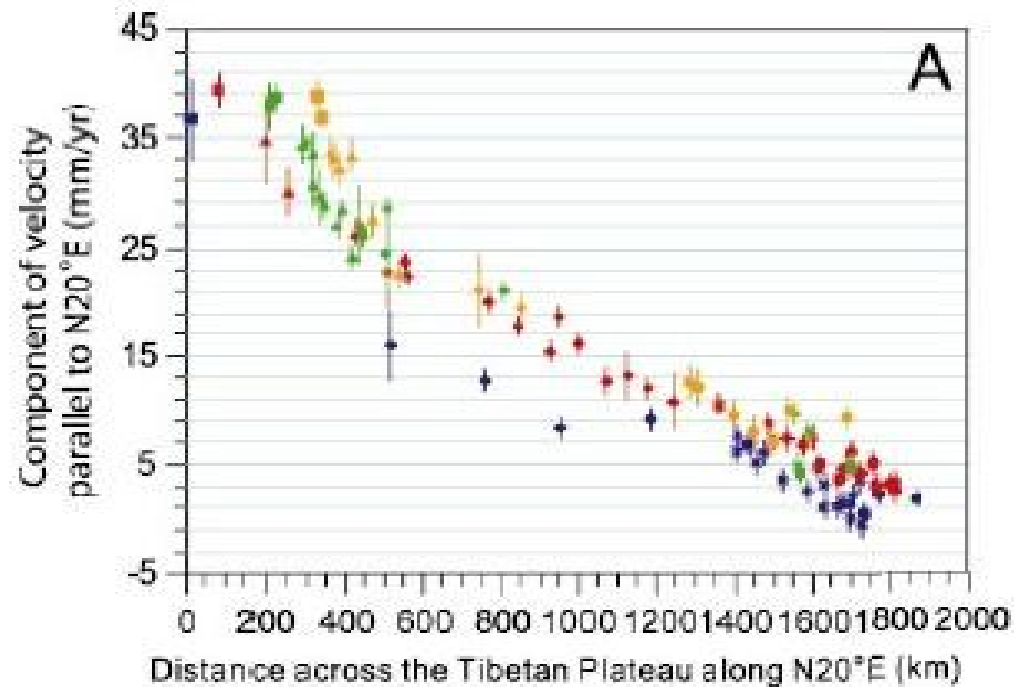
Indian-Asian collision  
modelled as a plastic layer  
deforming in plane-strain

Tapponnier et al. (1978)



# GPS displacement field across Tibet (Zhang et al., Geology, 2004)

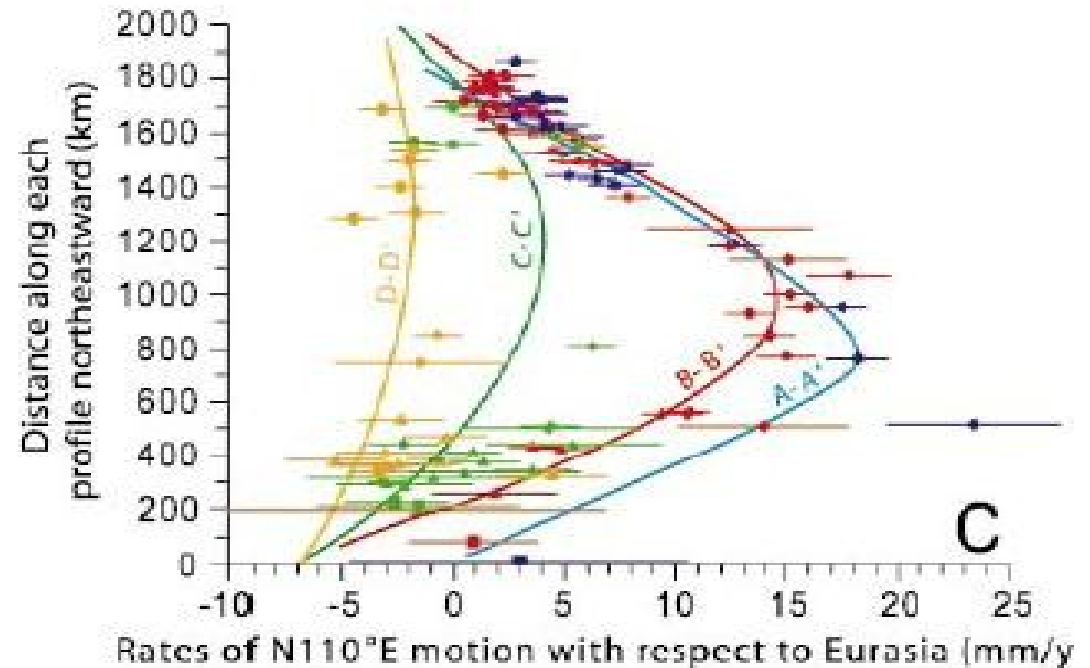




Motion in direction N20°E

GPS displacements on profiles across the major faults of Tibet (Zhang et al., Geology, 2004)

Motion in direction N110°E



## Continuum vs Block models

Faults appear to be an important element of the deformation field in Tibet, but the apparently continuous variation of the gps displacement field implies that movement on the faults is controlled by gradual deformation of an underlying viscous layer which probably supports the stress field.

Assuming continuum deformation therefore may be a better strategy than it seems on first evidence.

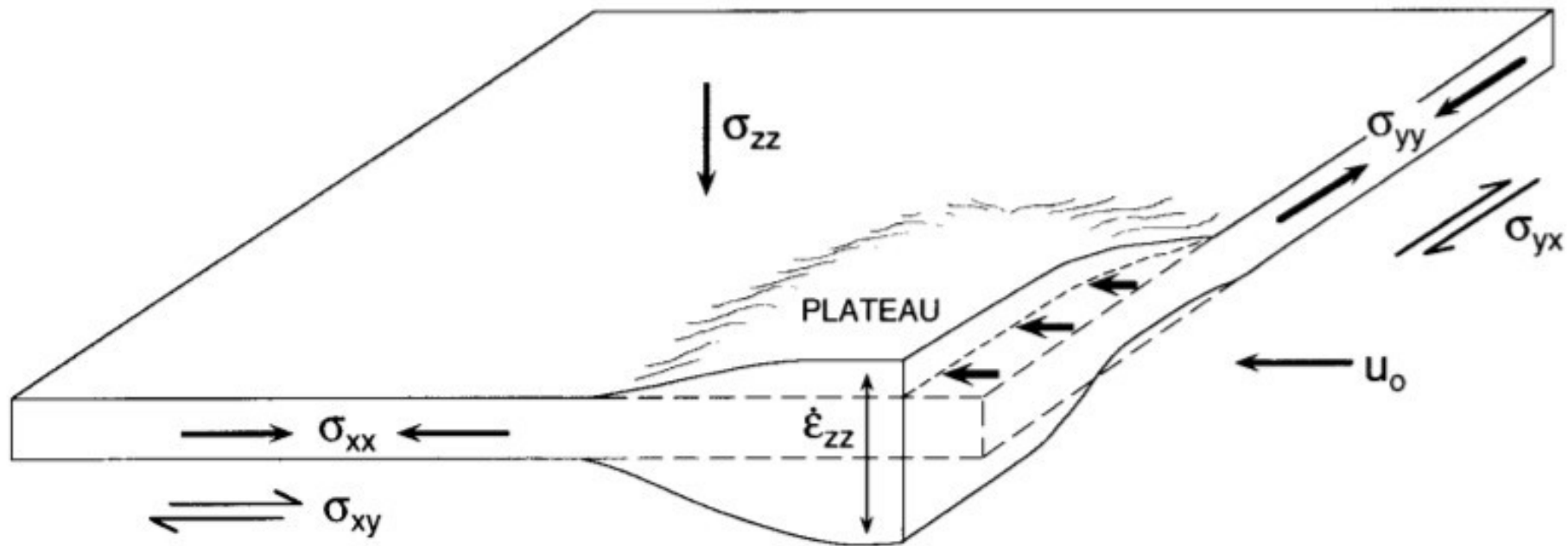
Faults may be superficial features, accommodating strain in the uppermost layers, without having a major effect on the overall continuum strain distribution.

A continuum deformation model must also recognise the basic geometrical constraints on the problem: the lithosphere is ~ 100 km thick, but the deformation field of Central Asia extends several thousand km across Tibet and Mongolia.

# Thin Viscous Sheet Model - Assumptions

The lithosphere is represented as a thin layer within which the horizontal displacement rates ( $u, v$ ) are constant with depth.

We assume local isostasy, with vertical tractions on vertical planes also set to zero.



## Thin Viscous Sheet Model - Assumptions

Flow is driven by external boundary tractions and by internal gradients of gravitational potential energy

Horizontal stress is averaged over the thickness of the layer.

Vertical columns of material in the layer are transported, thinned, thickened, or sheared horizontally, but they remain vertical columns.

The rate of thickening or thinning depends on the horizontal divergence of the displacement rate field.

$$\frac{1}{S} \frac{\partial S}{\partial t} = - \left( \frac{\partial u}{\partial x} + \frac{\partial v}{\partial y} \right)$$

The thin viscous sheet model provides a dynamically self consistent way to reduce the 3D lithospheric continuum deformation problem to 2D.

# Vertical Stress Balance

Vertical stress  $\sigma_{zz}$  is locally balanced (assuming isostasy).

$$(\nabla \cdot \boldsymbol{\sigma})_z = \frac{\partial \sigma_{xz}}{\partial x} + \frac{\partial \sigma_{yz}}{\partial y} + \frac{\partial \sigma_{zz}}{\partial z} = g \rho \quad \sigma_{zz} = - \left( g \rho_m L \right) \int_{z'}^{1+e'} \rho' d\zeta'$$

In the thin sheet formulation we remove the vertical dimension by averaging everything over the thickness  $L$  of the lithosphere. The isostatic condition then provides the depth-averaged vertical stress:

$$\bar{\sigma}_{zz} = - \left( g \rho_m L \right) \int_0^{1+e'} \int_{z'}^{1+e'} \rho' d\zeta' dz' = - \left( g \rho_m L \right) \int_0^{1+e'} \rho' z' dz'$$

You can interpret this integral as the integrated gravitational potential energy of the lithospheric column, and we can evaluate this integral approximately for an isostatic model with constant density crust (thickness  $S$ ) over constant density mantle:

$$\nabla \text{GPE} \propto \nabla S^2$$

Simplified density model (constant density crust and mantle):

$$\rho' = 1 \quad 0 \leq z \leq (1 + e - h)$$

$$\rho' = \rho_c' \quad (1 + e - h) \leq z \leq (1 + e)$$

Gravitational potential energy evaluates to:

$$\bar{\sigma}_{zz} = - \left( g \rho_m L \right) \left( \int_0^{1+e'-S'} z \, dz + \int_{1+e'-S'}^{1+e'} (z \rho_c') \, dz \right)$$

lots of algebra..... then use isostasy to eliminate  $e'$ :

$$e' = (1 - \rho_c') (S' - S'_0)$$

lots more algebra.....

$$\bar{\sigma}_{zz} = - \left( g \rho_m L \right) \left[ 1 - 2(1 - \rho_c') S_0 + (1 - \rho_c')^2 S_0^2 + \rho_c' (1 - \rho_c') S^2 \right]$$

and:

$$\nabla \bar{\sigma}_{zz} = \frac{-g \rho_c}{2L} \left( 1 - \frac{\rho_c}{\rho_m} \right) \nabla S^2$$

## Horizontal Stress Balance

In the horizontal direction the pressure takes the role of a body force:

$$(\nabla \cdot \underline{\tau})_x = \frac{\partial \bar{\tau}_{xx}}{\partial x} + \frac{\partial \bar{\tau}_{xy}}{\partial y} + \cancel{\frac{\partial \bar{\tau}_{xz}}{\partial z}} = -\frac{\partial \bar{p}}{\partial x} = -\frac{\partial \bar{\sigma}_{zz}}{\partial x} + \frac{\partial \bar{\tau}_{zz}}{\partial x}$$

We replace the pressure in this vertically averaged equation using the vertical stress (GPE) and vertical deviatoric stress (known in terms of the horizontal velocity gradients).

$$\frac{\partial}{\partial x} (2\eta \dot{\epsilon}_{xx}) + \frac{\partial}{\partial y} (2\eta \dot{\epsilon}_{xy}) = -\frac{\partial \bar{\sigma}_{zz}}{\partial x} + \frac{\partial}{\partial x} (2\eta \dot{\epsilon}_{zz})$$

We substitute for the vertical component of strain, using the two components of horizontal strain (incompressible flow):

$$4\frac{\partial}{\partial x} (\eta \dot{\epsilon}_{xx}) + 2\frac{\partial}{\partial x} (\eta \dot{\epsilon}_{yy}) + \frac{\partial}{\partial y} (2\eta \dot{\epsilon}_{xy}) = -\frac{\partial \bar{\sigma}_{zz}}{\partial x}$$

## Horizontal Stress Balance

And replace the strain rates by gradients of displacement rate:

$$4 \frac{\partial}{\partial x} \left( \eta \frac{\partial u}{\partial x} \right) + 2 \frac{\partial}{\partial x} \left( \eta \frac{\partial v}{\partial y} \right) + \frac{\partial}{\partial y} \left[ \eta \left( \frac{\partial u}{\partial y} + \frac{\partial v}{\partial x} \right) \right] = \frac{g \rho_c}{2L} \left( 1 - \frac{\rho_c}{\rho_m} \right) \frac{\partial S^2}{\partial x}$$

Finally we non-dimensionalise, using,  $L$  for length,  $U_0$  for velocity, and  $\eta_0$  for viscosity

$$4 \frac{\partial}{\partial x} \left( \eta \frac{\partial u}{\partial x} \right) + 2 \frac{\partial}{\partial x} \left( \eta \frac{\partial v}{\partial y} \right) + \frac{\partial}{\partial y} \left[ \eta \left( \frac{\partial u}{\partial y} + \frac{\partial v}{\partial x} \right) \right] = \frac{Ar}{2} \frac{\partial S^2}{\partial x}$$

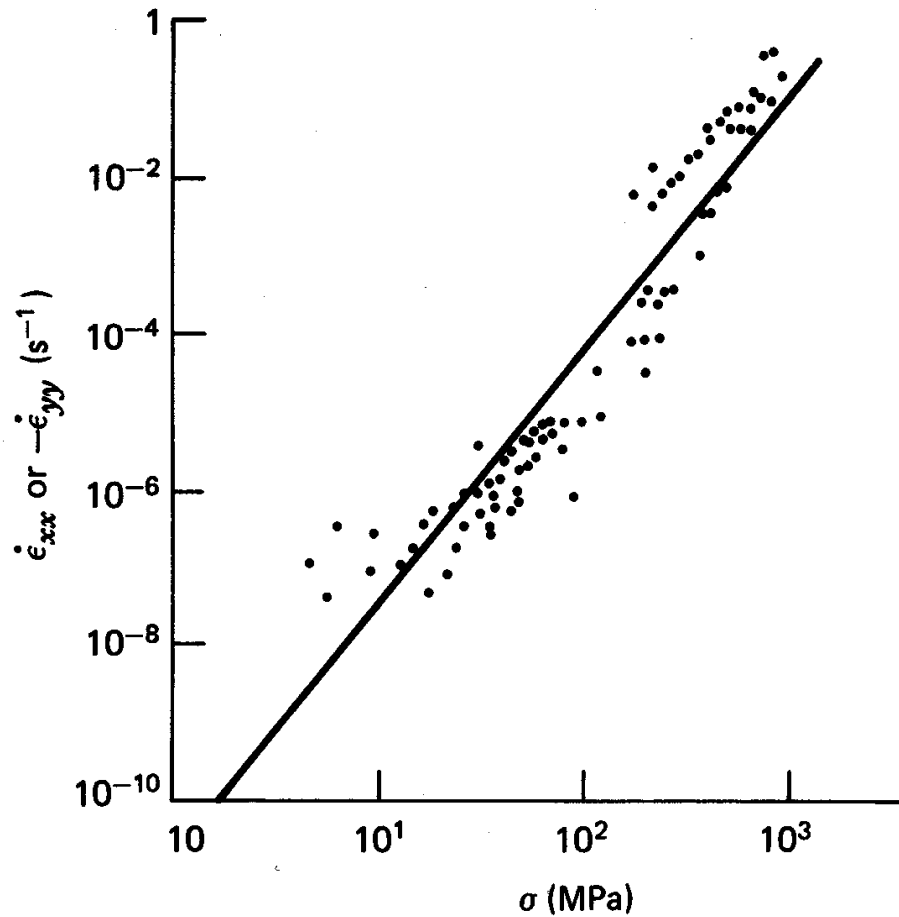
and similarly in the y-direction:

$$2 \frac{\partial}{\partial y} \left( \eta \frac{\partial u}{\partial x} \right) + 4 \frac{\partial}{\partial y} \left( \eta \frac{\partial v}{\partial y} \right) + \frac{\partial}{\partial x} \left[ \eta \left( \frac{\partial u}{\partial y} + \frac{\partial v}{\partial x} \right) \right] = \frac{Ar}{2} \frac{\partial S^2}{\partial y}$$

All the variables in this equation should now be considered dimensionless, and the remaining free variable is

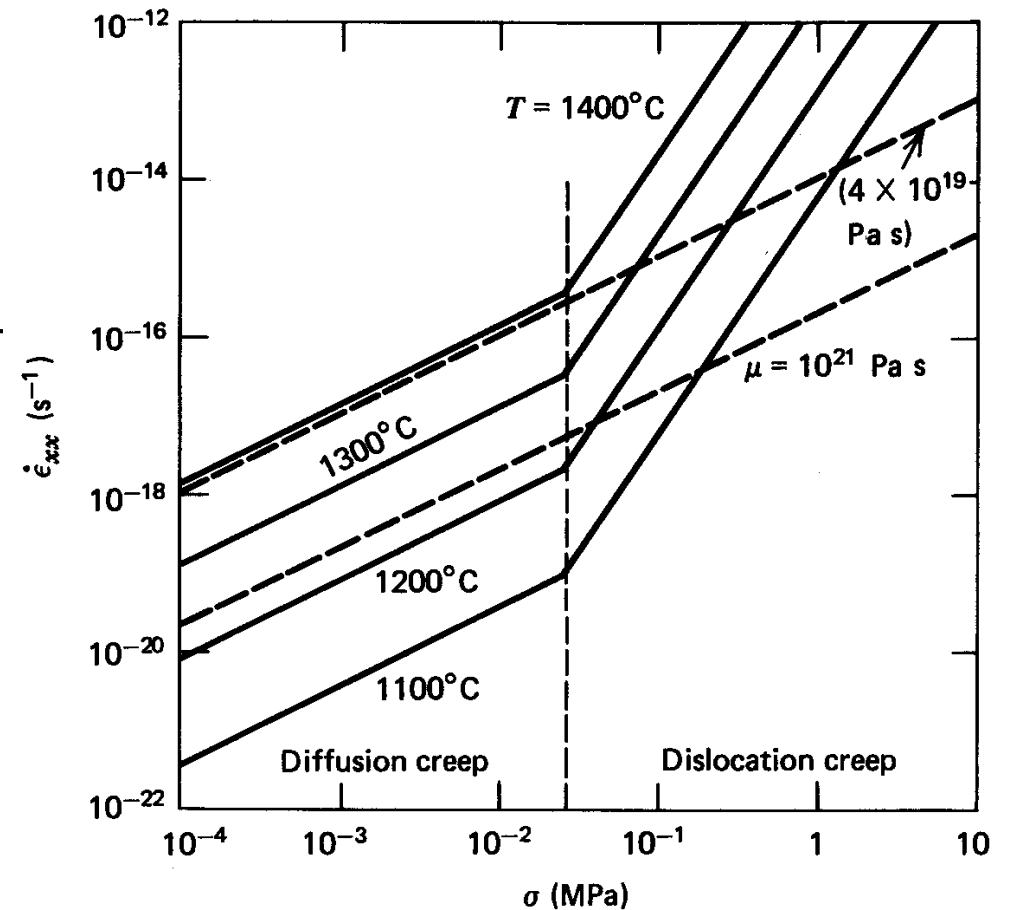
$$Ar = \frac{g \rho_c L}{\eta_0 (U_0 / L)} \left( 1 - \frac{\rho_c}{\rho_m} \right)$$

## Strain-rate vs stress



Experimental data for olivine at  $1400^\circ\text{C}$  with dislocation creep. The straight line has a slope of 3.

Diffusion creep is the dominant mechanism for low stress difference. At high stress difference, power-law creep dominates. Dashed lines show the apparent viscosities of asthenosphere and mantle.



# Non-Newtonian Constitutive Relation

For a power-law constitutive relation we can't just write

$$\dot{\epsilon}_{ij} = A (\tau_{ij})^n$$

but we can write a power law using the second invariant of the deviatoric stress:

$$\dot{\epsilon}_{ij} = A \Theta^{(n-1)} \tau_{ij} \quad \Theta = \sqrt{\sum_{ij} \tau_{ij} \tau_{ij}}$$

with some algebra we can invert this relation:

$$\tau_{ij} = B \dot{E}^{(1-n)/n} \dot{\epsilon}_{ij} \quad \dot{E} = \sqrt{\sum_{ij} \epsilon_{ij} \epsilon_{ij}}$$

which defines an effective (depth-averaged) viscosity:

$$\bar{\eta} = \frac{B}{2} \dot{E}^{(1-n)/n} \quad \eta_0 = B_0 (U_0/L)^{(1-n)/n}$$

providing the viscosity scale to be used in the Argand number:

$$Ar = \frac{g \rho_c L}{B_0 (U_0/L)^{1/n}} \left( 1 - \frac{\rho_c}{\rho_m} \right)$$

# Extrapolation of the Constitutive Law

- We measure the constitutive law directly for samples at the  $10^{-2}$  m scale at strain rates of around  $10^{-7}$  s $^{-1}$ , often at temperatures close to the homologous melting temperature.
- On that basis, we extrapolate across 6-8 orders of magnitude in space and time to construct a theory for deformation of the lithosphere at the continental length scale ( $10^6$  m) and the geological time scale ( $10^{13}$  s $^{-1}$ ).
- Extrapolation is uncertain because of possible changes in deformation mechanism and temperature, and the averaging of deformation in large inhomogeneous volumes.
- Keep in mind that the extrapolation may be unreliable. It is a better scientific strategy to assume the lithospheric properties are not known reliably and to use the techniques of numerical experiment to constrain the parameters in the effective constitutive law.

# Argand Number

For non-Newtonian viscosity

$$Ar = \frac{g \rho_c L}{B_0 (U_0 / L)^{1/n}} \left( 1 - \frac{\rho_c}{\rho_m} \right)$$

Ar is named after Emile Argand, who described (1924) in general terms the deformation that has evidently occurred in Central Asia.

The Argand number (England and McKenzie, 1982) indicates the relative magnitude of buoyancy forces (gradients of potential energy produced by crustal thickness variation) to viscous stress (produced by the indentation of a boundary at rate  $U_0$ ).

Apart from geometrical factors describing the domain, and internal variation of parameters such as  $B$ , the calculation is controlled just by two key parameters:  $n$  and  $Ar$

We could just assume  $n$  and  $Ar$  using a priori information, or we could use numerical experiments to estimate them.

## Thin Viscous Sheet Solution Method (*basil*)

Velocity fields  $u(x,y)$ ,  $v(x,y)$  are represented on the  $(x,y)$  domain using a quadratic interpolation field on an individual triangular area element

$$u(x, y) = \sum_{j=1}^6 U_j N_j(x, y)$$

where  $N_j$  is the quadratic interpolation point. We construct a 2D mesh of such triangles, and use the finite element method (Galerkin weighting) to assemble a matrix equation like:

$$\begin{bmatrix} K_{xx} & K_{xy} \\ K_{yx} & K_{yy} \end{bmatrix} \begin{bmatrix} U \\ V \end{bmatrix} = \begin{bmatrix} a \\ b \end{bmatrix}$$

where the elements of  $K_{ij}$  describe the stiffness of the elements (incorporating viscosity), the  $(a_i, b_i)$  incorporate the GPE gradients and boundary tractions, and we solve this matrix equation for the values of the nodal velocity components  $[U, V]$ , using the conjugate gradient method.

## India-Asia Collision

Indian subcontinent collided with Central Asia at about 50 Ma, after separating from Gondwanaland and moving rapidly from the southern hemisphere.

Since 50 Ma India continues to move northwards at about 4.5 cm/yr.

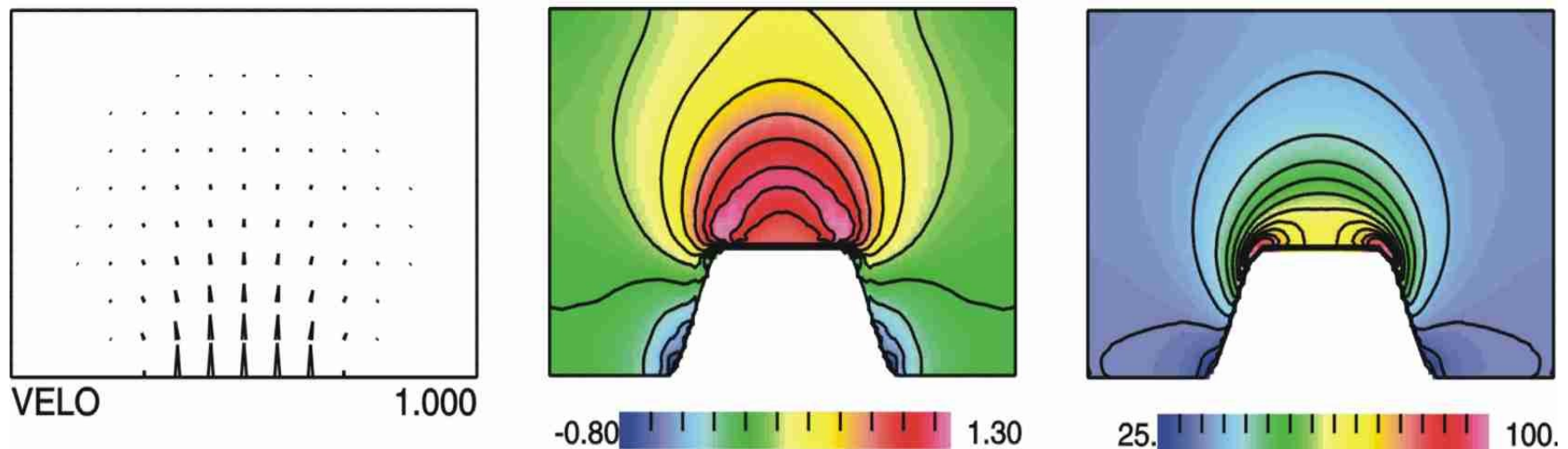
Major consequences:

Formation of major mountain ranges: Himalaya, Tian Shan, Karakoram

Tibetan Plateau (approximately 2000 km by 2500 km)  
crustal thickness doubled to about 80 km.

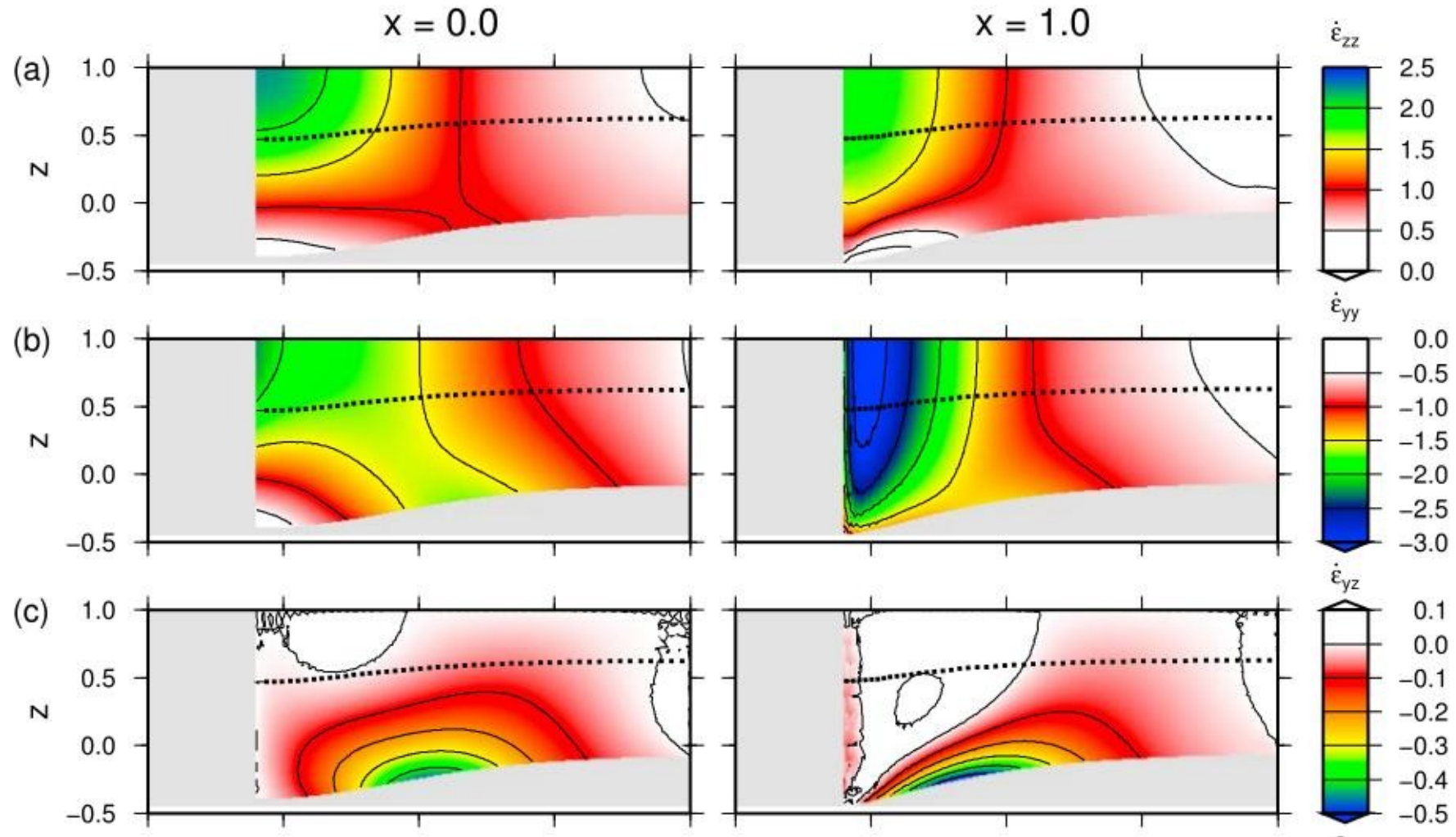
## Indenting Boundary with $n = 3$

- The collision of India with Asia over the past 50 Myr provides the classic example of deformation induced by a convergent boundary condition
- $n=1$  predicts a much broader zone of deformation than is observed.
- $n=3$  at least localizes deformation within about 2000 km of the boundary.
- Buoyancy forces ( $Ar = 1$ ) cause plateau to build outward on the north



velocity field at  $t = 0$ , vertical strain-rate (% Myr<sup>-1</sup>) and crustal thickness (km relative to initial uniform 35 km thick layer) shown after 50 Myr.

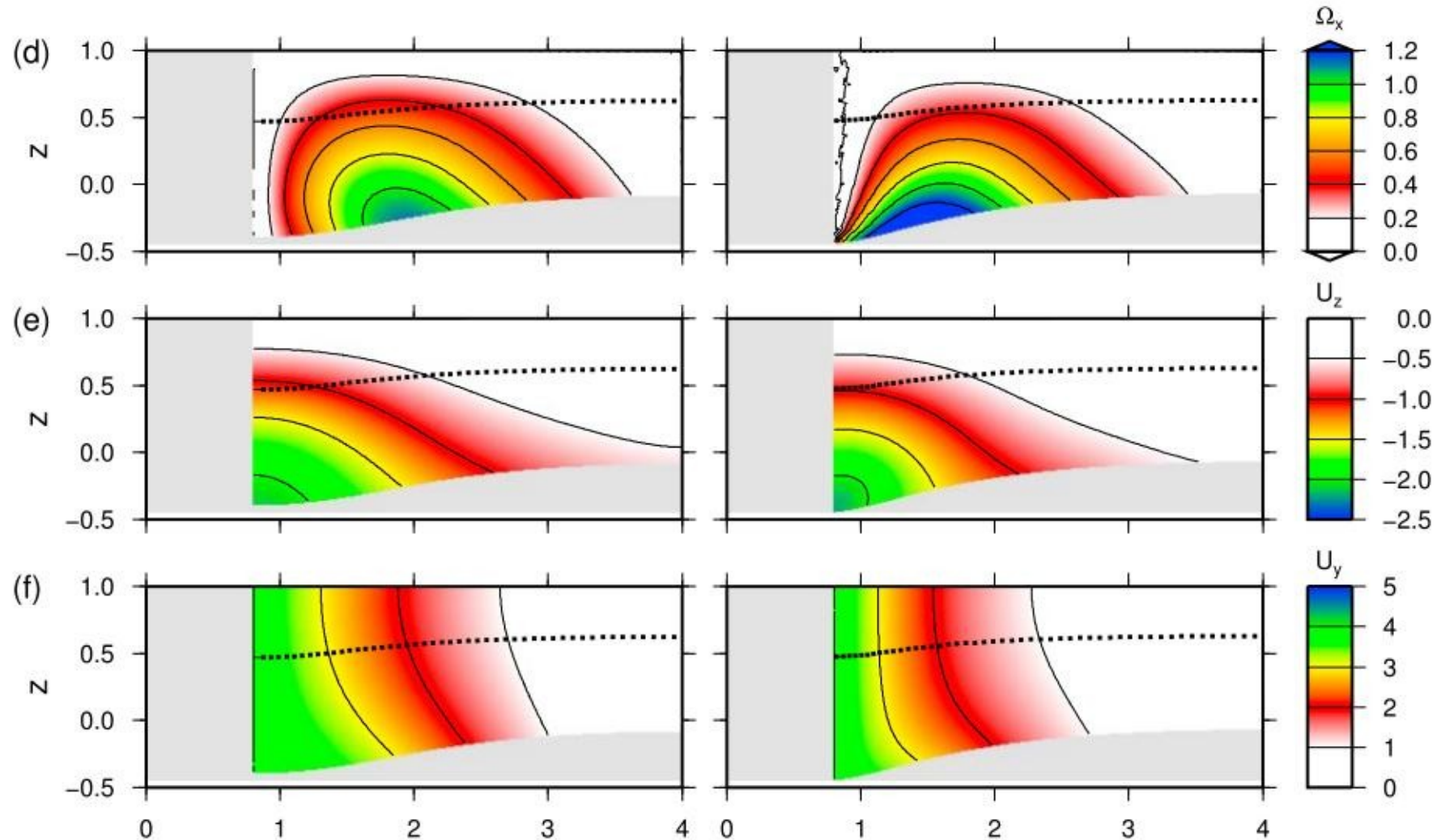
# How accurate is the Thin Viscous Sheet approximation?



Compare 2D TVS vs 3D constant properties:

$n = 3$ ,  $Ar = 0$ ,  $D/L = 1$ ,  $t' = 0.2$ , sliding top, free bottom  
Garthwaite and Houseman, *JGR*, 2010.

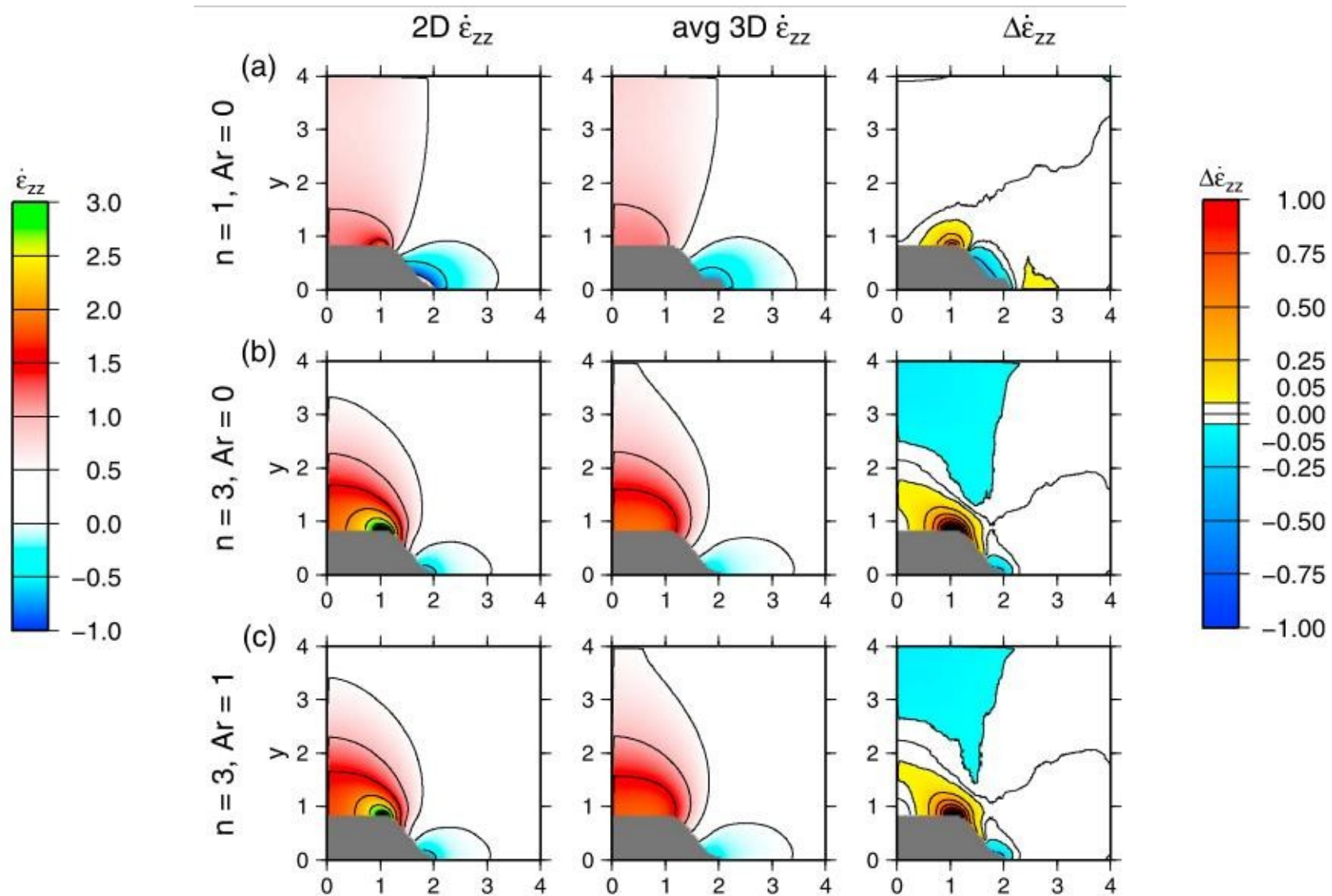
## How accurate is the Thin Viscous Sheet approximation?



Compare 2D TVS vs 3D constant properties:

$n = 3$ ,  $Ar = 0$ ,  $D/L = 1$ ,  $t' = 0.2$ , sliding top, free bottom  
Garthwaite and Houseman, *JGR*, 2010.

# How accurate is the Thin Viscous Sheet approximation?



Compare 2D TVS vs 3D,  $D/L = 1$  (Garthwaite and Houseman, *JGR*, 2010)

## Strength Variations in the Layer

Strength variations, represented by the parameter  $B$  in the viscous constitutive relation may be caused by geothermal variation, or prior history of deformation.

A strong region, such as the Tarim Basin may act as a secondary indenter, transmitting and refocusing the stress caused by the primary indenter to cause a second region of thickening (the Tien Shan).

Variations in the strength coefficient are amplified if  $n > 1$ . Stress varies as

$$\tau \approx B \dot{\epsilon}^{1/n}$$

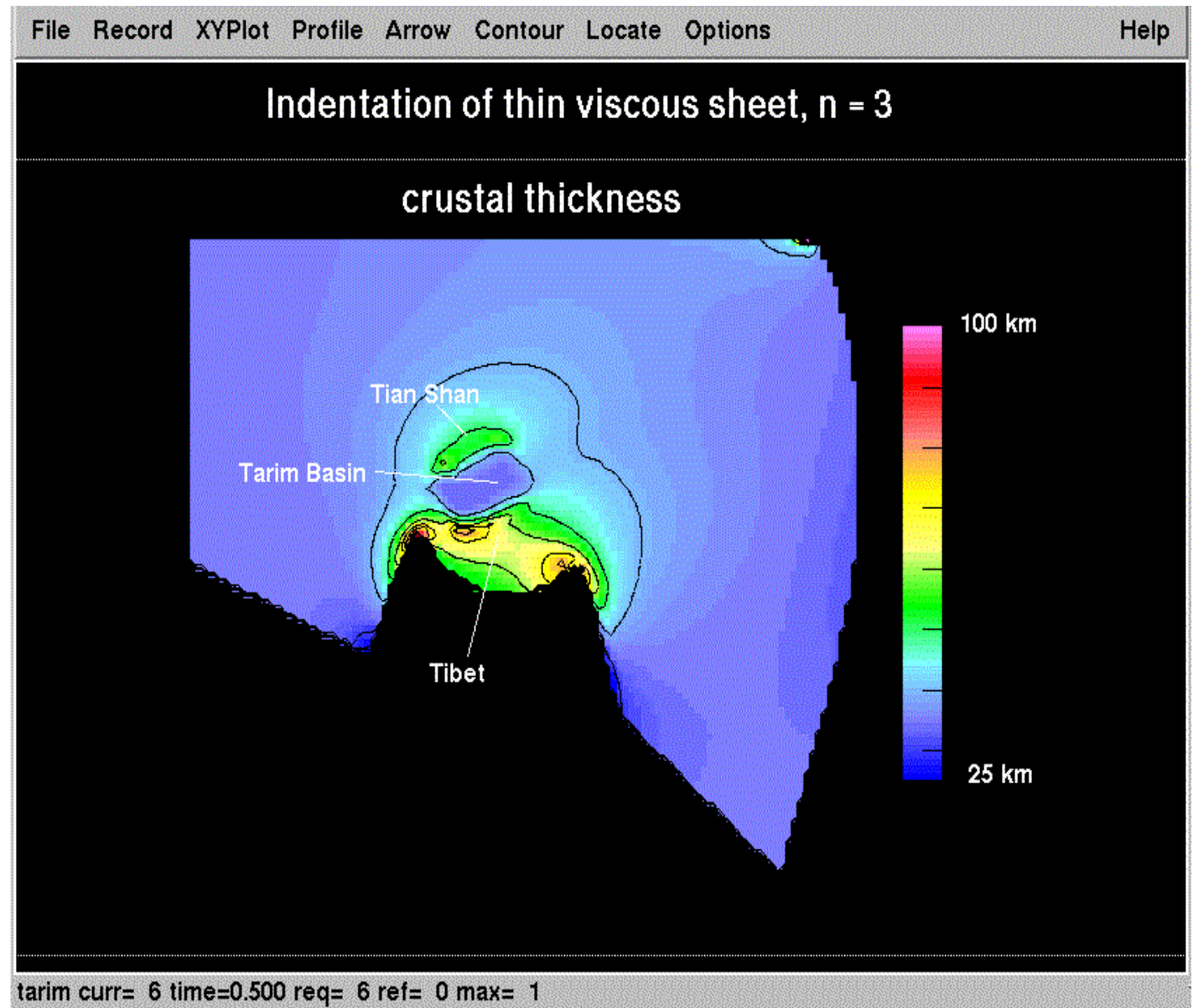
doubling  $B$  for example may cause a factor of 8 decrease in  $\dot{\epsilon}$  if  $n = 3$ , under a constant driving stress.

discontinuities in the viscous strength coefficient may cause shear strain to be localised.

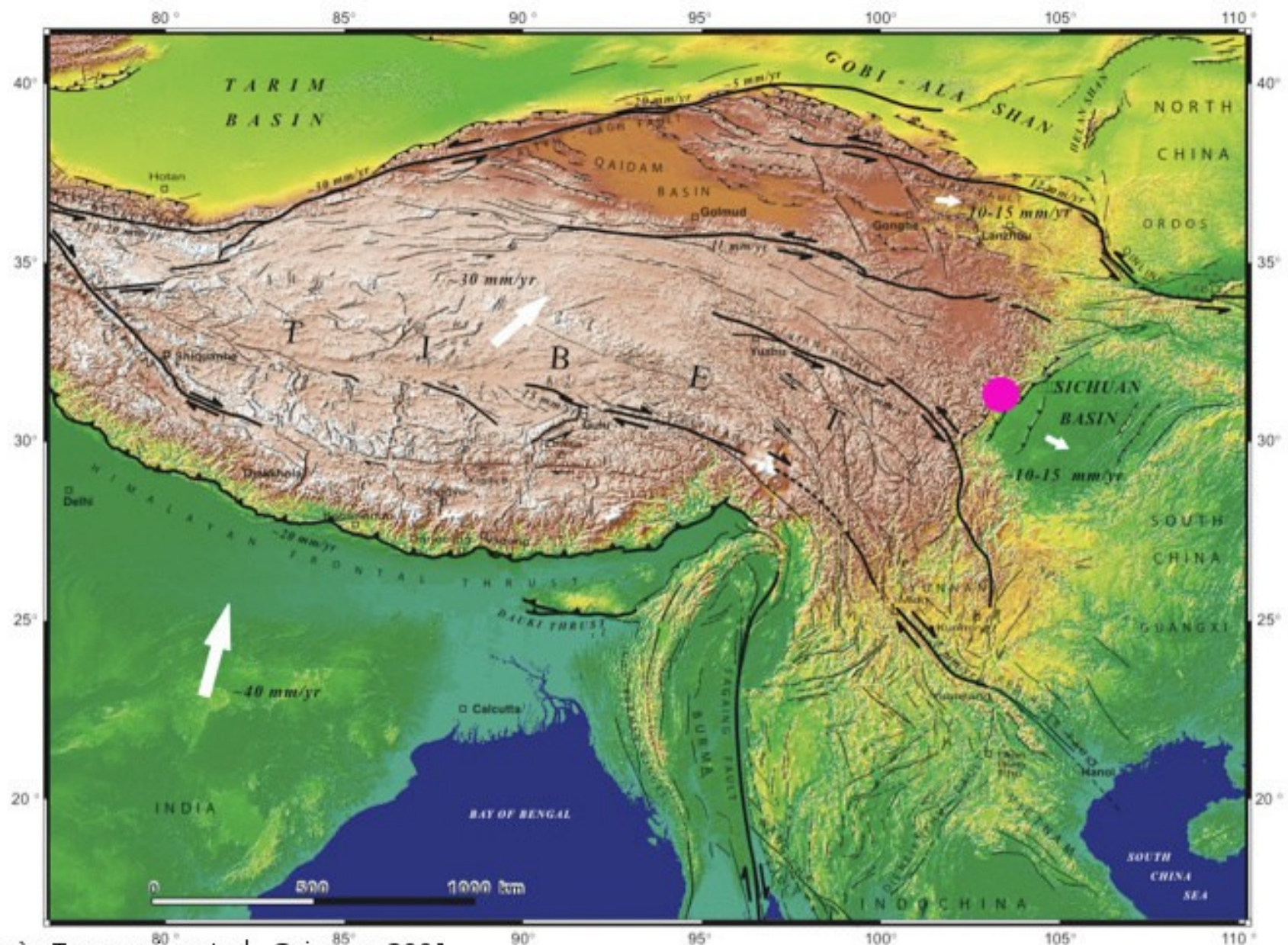
## Indian-Asian collision: thin sheet simulation

Asymmetric boundary conditions and variation of the viscous strength coefficient of the thin sheet allow a more realistic representation.

The Tarim Basin appears to act as a secondary indenter, focussing deformation into the region of the Tien Shan.



## Topography and major faults in Tibet

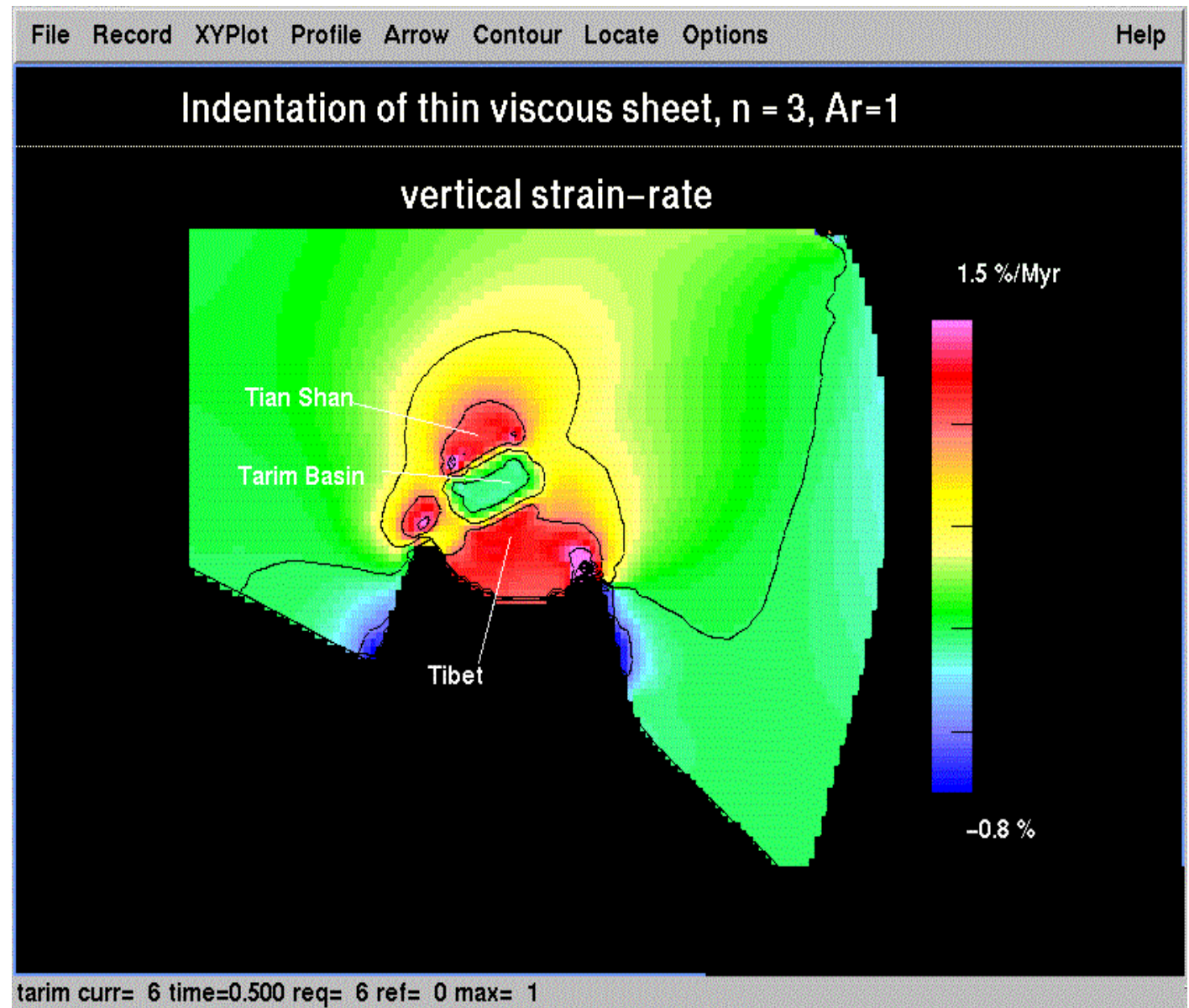


d'après Tapponnier et al., Science, 2001

## Convergence implies thickening ?

If convergence continues at a steady rate, then thickening also must continue in the simple version of the thin viscous sheet model.

Tibet is now extending, even though the convergence continues, pointing to one limit on the validity of the thin sheet model.



## Plateau Evolution

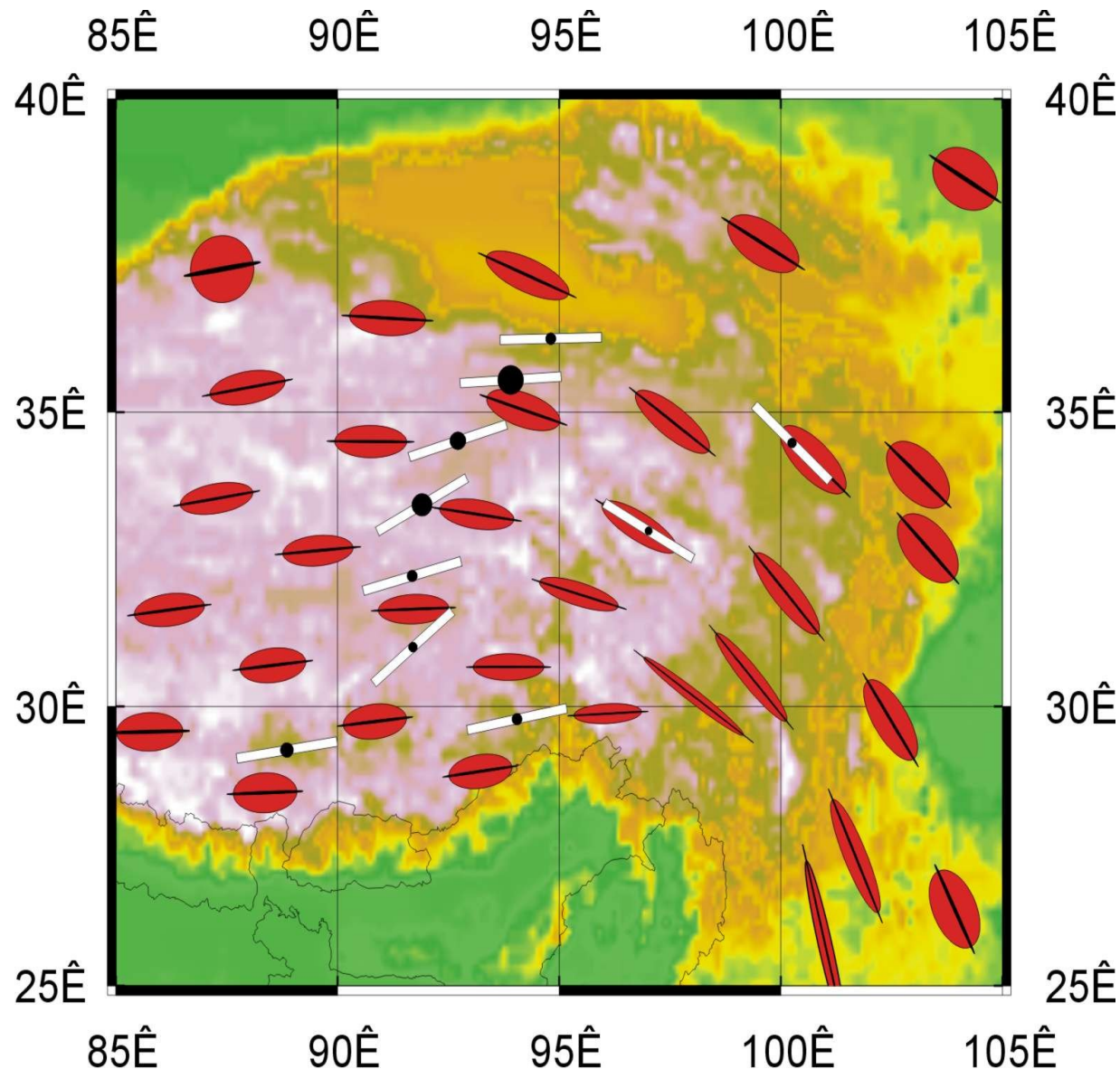
Numerical experiments suggest that plateau grows during collision by crustal thickening on its outer perimeter.

Locus of maximum deformation moves northward during the collision.

Most of present crustal thickening and seismic activity in Indian-Asian collision occurs to the north and east of Tibet. Tian Shan range in western China is probably location of maximum crustal thickening rates today.

At about 15 Ma, N-S compression of Tibet was replaced by E-W extension. At same time plateau elevation increased dramatically.

## Prediction of fast S-wave polarisation



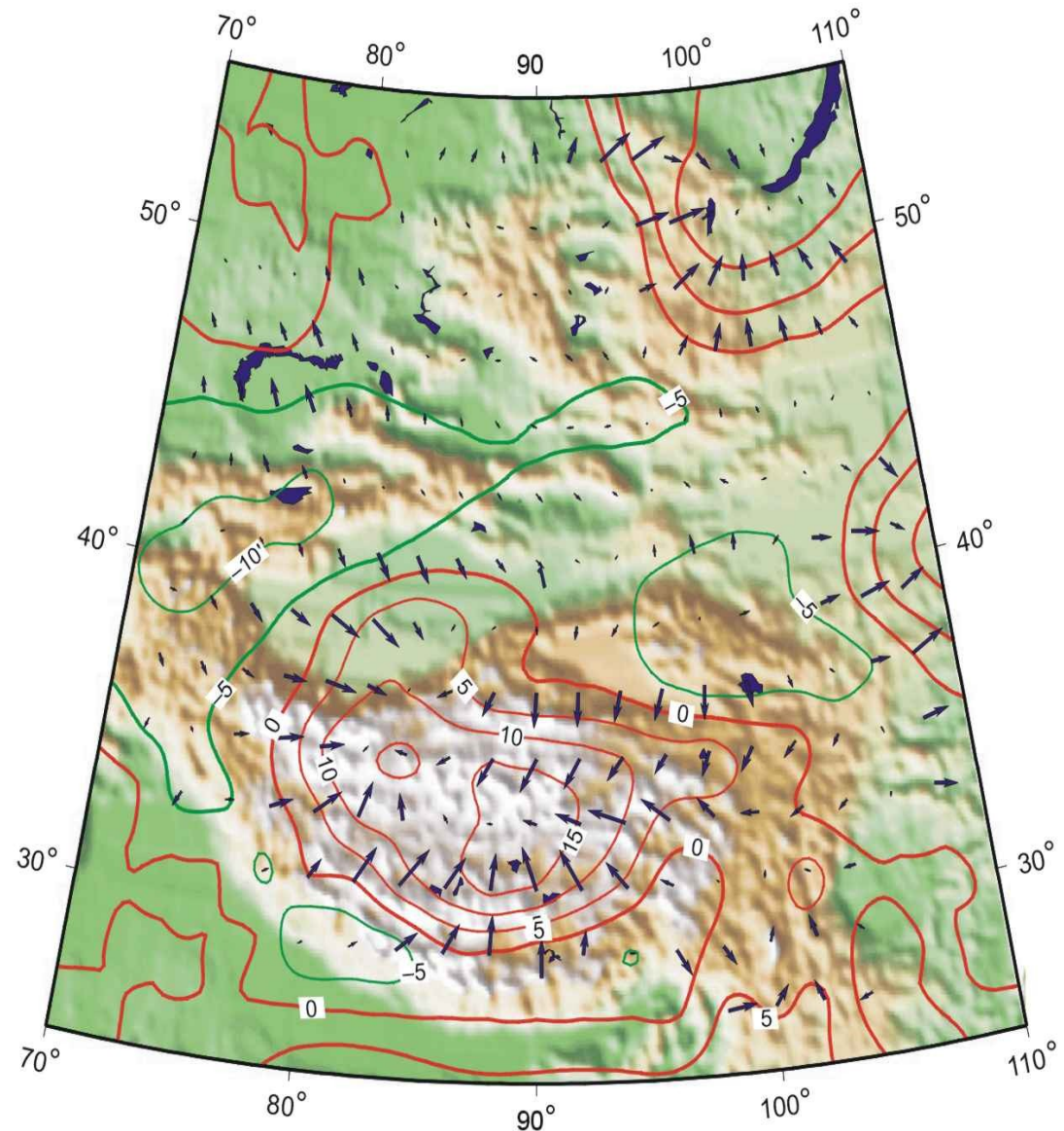
Shortening directions predicted by the finite strain ellipses determined from the finite element calculations provide a partial test of the thin viscous sheet model.

Fast SKS directions are expected to align with the elongation axes of the finite strain ellipses that show the accumulated finite strain (assumed coherent through the lithosphere).

# Potential Energy Gradients

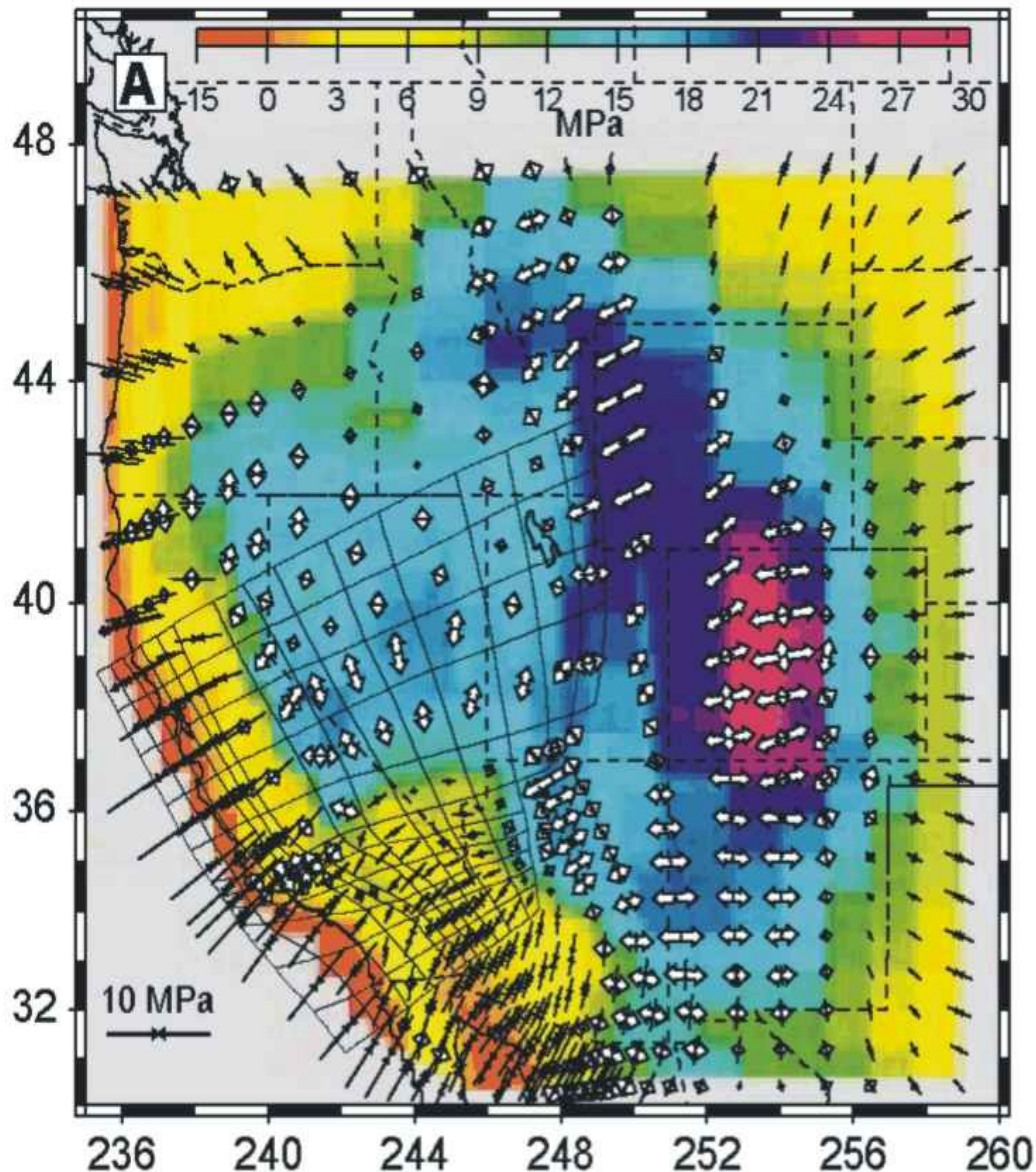
A test of the thin sheet model: England and Molnar (1997) showed that the gradients of GPE (blue arrows) could be inferred from the gradients of viscous stress that are calculated from the strain-rate field measured using earthquakes and recent faults, and an assumed non-linear viscous constitutive law.

They inferred that the effective viscosity of the lithosphere is  $\sim 10^{22}$  Pa s.



$$\nabla \cdot \mathbf{\tau} - \nabla \bar{\tau}_{zz} = -\nabla \bar{\sigma}_{zz} = \frac{Ar}{2} \nabla S^2$$

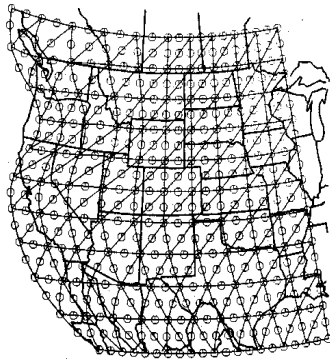
## GPE-derived Stress Field - southwest USA



Flesch et al, (Science, 2000) calculated gradients of GPE derived from topographic and geoid data to predict one component of the deformation field in the southwestern USA. In combination with the stress field produced by relative movement of the adjacent Pacific Plate, the predicted stress directions and strain-rate magnitudes agree with those observed for effective lithospheric viscosity around  $10^{22}$  Pas ( $10^{21}$  Pas in California shear zone)

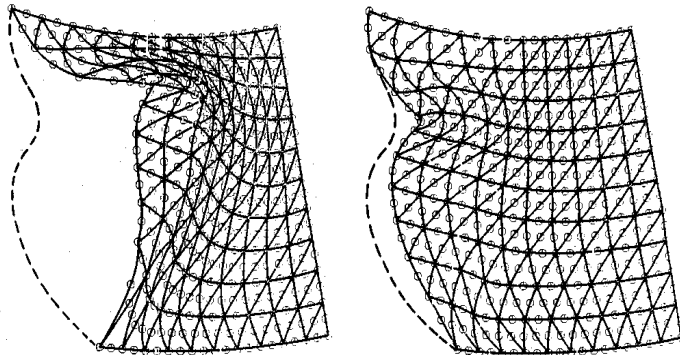
The magnitude of stress is determined directly by GPE.

## Two layer models of Indentation of western USA



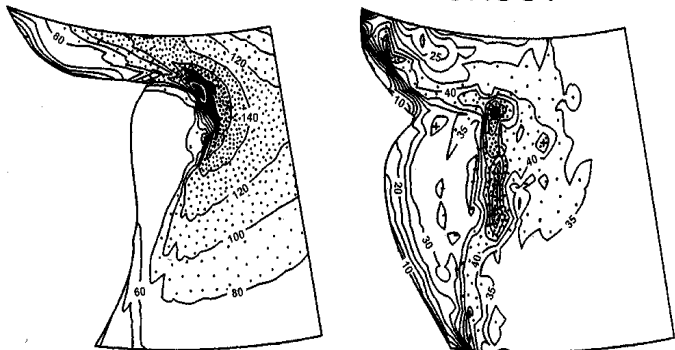
Bird (1989) modelled the orogenesis of the western US, allowing for the possibility that crust and mantle are decoupled by a low strength layer at the base of the crust

Buoyancy of the crust combined with its low strength prevents the crustal layer from thickening to the same degree as the mantle layer.

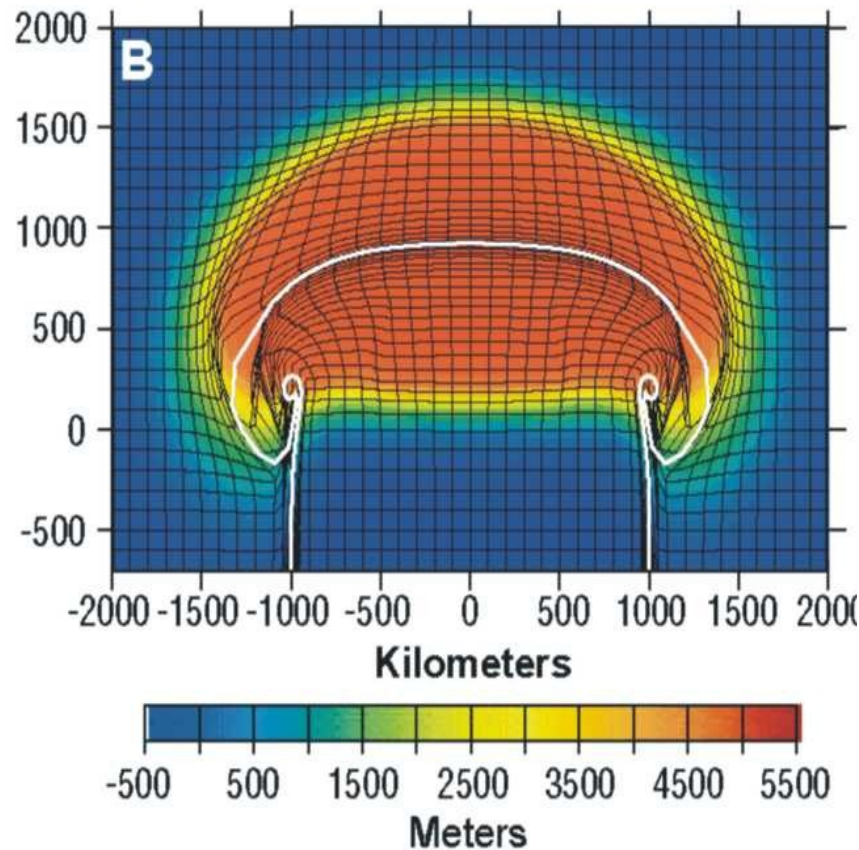


MANTLE

CRUST

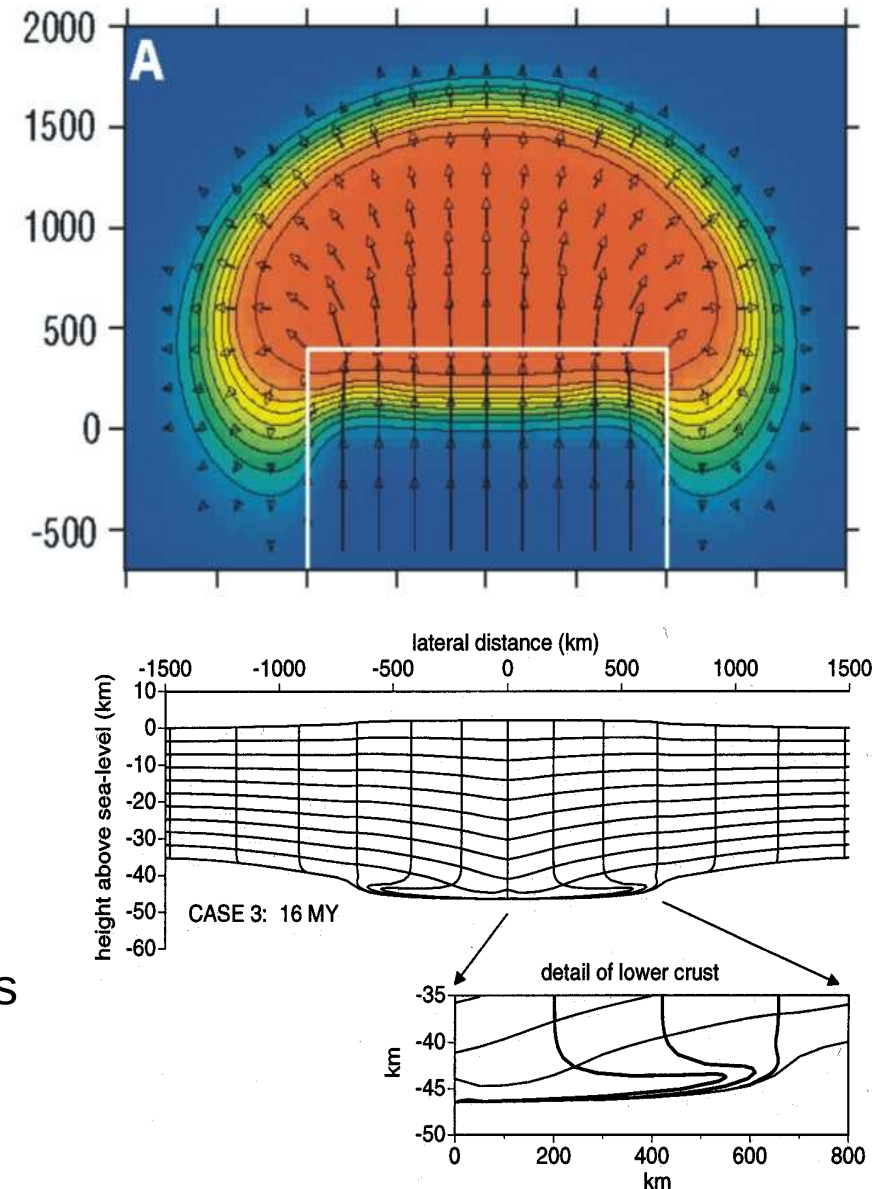


## A low viscosity layer in lower crust spreads faster ?



Royden (1996), Royden et al. (1997), and Shen et al (2001) argue that a low viscosity lower crust is required to explain the flatness of the plateau.

(250 m of  $10^{12}$  Pa s, or 15 km of  $10^{18}$  Pa s).



## Low Viscosity crust + Erosion

Avouac and Burov (1996) also argued for a low viscosity layer at the base of the crust - if the strength of this layer is based on a quartz deformation law.

Under these conditions they suggested that a 3 km high range should spread gravitationally, but that plausible erosion rates could in fact cause inward flow beneath the topographic heights, enhancing and localizing the convergence.

